

## PHASE BEHAVIOR OF AMPHIPHILIC SYSTEMS\*

U.S. SCHWARZ

Max-Planck-Institut für Kolloid- und Grenzflächenforschung  
Kantstr. 55, 14513 Teltow, Germany*(Received April 21, 1998)*

Due to the enormous complexity of amphiphilic systems on microscopic scales, their modelling often starts from mesoscopic length scales. In recent years Ginzburg–Landau theories and curvature models have fostered considerable progress in understanding different aspects of binary and ternary amphiphilic systems. We have investigated to what extent these models can be used to understand amphiphilic phase behavior. It is argued that Ginzburg–Landau model are well suited to describe ordered phases at low temperatures. A Ginzburg–Landau model for binary amphiphilic systems is presented which yields the typical phase sequence disordered micellar–micellar cubic–hexagonal–lamellar–bicontinuous cubic–inverted hexagonal–inverted micellar cubic–disordered inverted micellar, which is observed experimentally. At higher temperatures fluctuation effects become more important, and lamellar and sponge phases/microemulsions are favored. It is argued that curvature models which include fluctuation effects and long ranged interactions like steric or van der Waals interactions are more suited to predict amphiphilic phase behavior in this case. It is shown that such a model can explain, for example, that in ternary systems the lamellar phase often extends far into the water apex when the phase inversion temperature is approached from below.

PACS numbers: 82.65. Dp, 82.70. -y, 64.70. Md, 61.30. Cz

**1. Introduction**

Amphiphiles are molecules which have both non-polar and polar parts [1]. Special cases of amphiphilic systems are tensides which are used for all kinds of washing and emulsification purposes and lipids which build up biological membranes. Regarding amphiphilic phase behavior, tenside systems with polyoxyethylenes  $C_iE_j$  are particularly well investigated experimentally.

---

\* Presented at the Marian Smoluchowski Symposium on Statistical Physics, Zakopane, Poland, September 1–10, 1997.

Here  $C_i = \text{H}(\text{CH}_2)_i$  stands for the non-polar polyethylene part and  $E_j = (\text{OCH}_2\text{CH}_2)_j\text{OH}$  for the polar polyethylene oxide part [2–5].

In polar solvents like water, amphiphiles succeed in shielding non-polar parts from the solvent by self-assembling into amphiphilic aggregates like micelles and bilayers. In the case of spherical micelles, for example, the hydrophobic parts are located inside the globules and the hydrophilic ones form a spherical shell which faces the aqueous solvent. For small water concentrations, one might find inverted micelles with the hydrophobic parts outside and the water inside. Adding a non-polar component like oil to a binary system leads to a ternary system with the oil incorporated within the hydrophobic regions. Now the basic building blocks are not micelles and bilayers, but monolayers between polar and non-polar regions forming *e.g.* oil-filled micelles.

Binary as well as ternary amphiphilic systems generically feature an amazing degree of polymorphism due to the very small differences in free energy between the various structures. This means that structural changes can occur not only as a function of temperature, but also as the composition of the system is varied. In order to classify the different amphiphilic phases, we distinguish between micellar and non-micellar phases as well as between ordered and disordered phases. Micellar phases consist of spherical, cylindrical or plate-like amphiphilic aggregates which are disordered at low amphiphile concentration and pack into ordered phases at high amphiphile concentration. This includes the micellar disordered phase  $L_1$ , the micellar cubic phase  $I_1$ , the hexagonal phase  $H_1$  and the lamellar phase  $L_\alpha$ . Fig. 1(a) depicts the different geometries of micellar phases. Non-micellar phases consist of amphiphilic sheets (mono- or bilayers) which extend throughout the whole sample. Since they thereby divide it into two intertwined labyrinths which both can be used to traverse the sample in any arbitrary direction, they are also called *bicontinuous*. Non-micellar disordered phases include the sponge phase in binary and the microemulsion in ternary systems. Non-micellar ordered phases in most cases have cubic symmetry and are then denoted by  $V_1$ . Fig. 1(b) depicts the different geometries of non-micellar phases. Inverted versions of all structures are denoted by the index 2. For example the inverted hexagonal phase is  $H_2$ .

The main driving force for amphiphilic self-assembly is the hydrophobic effect which is very difficult to model on microscopic length scales. Therefore the modelling of amphiphilic systems often starts on mesoscopic length scales where one can make use of effective properties which are common to all amphiphilic systems [6]. In this contribution we discuss two model classes which have been proven to be very useful for studies of amphiphilic phase behavior: curvature models, which start from the effective properties of the amphiphilic interfaces, and Ginzburg–Landau models, which start from the

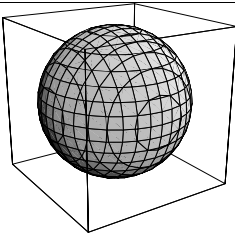
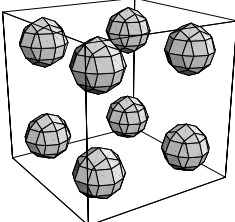
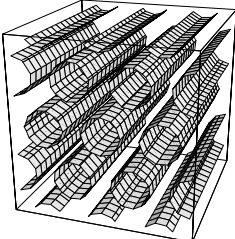
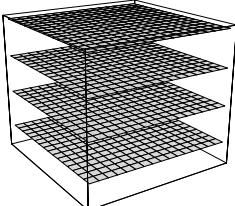
disordered spheres		micellar disordered phase $L_1$
packed spheres		micellar cubic phase $I_1$
packed cylinders		hexagonal phase $H_1$
packed planes		lamellar phase $L_\alpha$

Fig. 1(a). Geometries of micellar phases, where the amphiphile is constrained to micellar aggregates. The micellar disordered phase  $L_1$  consist of disordered spherical micelles. The micellar ordered phases consist of packed amphiphilic aggregates: spherical micelles form the micellar cubic phase  $I_1$ , cylindrical micelles the hexagonal phase  $H_1$  and plate-like micelles the lamellar phase  $L_\alpha$ . Note that the geometries are the same for binary and ternary systems; they differ in whether the micelles are filled with oil or not.

symmetries of order parameter fields which arise when averaging molecular densities over small regions of space. In comparing their respective virtues, we want to show that these two approaches are complementary to each other. Since typical energies are of the order of  $k_B T$ , the theoretical description of amphiphilic systems in both cases centers around the roles of geometrical structure and thermal fluctuations. Although there has been much work on

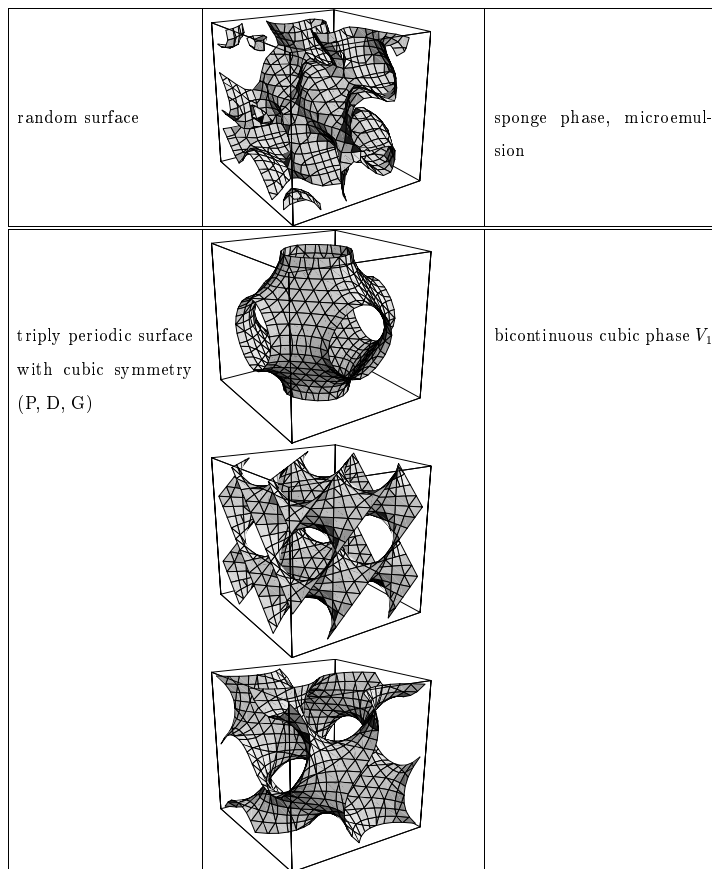


Fig. 1(b). Geometries of non-micellar or bicontinuous phases, where one amphiphilic sheet extends throughout the whole sample. As with micellar phases, the geometries are the same for binary and ternary systems, the difference being whether one has mono- or bilayers. The disordered phases are the sponge phase for binary and the microemulsion for ternary systems. Both can be modeled by random surfaces. Ordered bicontinuous phases normally have cubic symmetry. They can be modeled by triply periodic surfaces with cubic symmetry like the triply periodic minimal surfaces P, D and G which are shown. The latter two structures correspond to the double diamond and gyroid structures, respectively.

amphiphilic phase behavior in the framework of microscopic lattice models [6–8], in this contribution we focus on mesoscopic continuum models only.

In binary systems, bilayer structures can be modeled by using the curvature model. However, micellar structures have to be treated separately. Therefore curvature models are particularly suited when studying ternary systems since here all structures are build from monolayers. Thus with the

curvature model all relevant structures can be modeled on the same footing. It has been shown that a simple curvature model is sufficient to predict the typical phase sequence which one finds experimentally in ternary systems with water, polyoxyethylenes and alkanes when increasing the amphiphile concentration: spheres, cylinders, bicontinuous cubic structures, lamellae [9]. However, since this model is not thermodynamically stable, it does not give a thermodynamically correct phase diagram. Therefore we studied a curvature model which also considers fluctuation effects and van der Waals-interaction [10]. In the second section, we will report on results for the disordered micellar phase  $L_1$  and the lamellar phase  $L_\alpha$ . It will be demonstrated that apart from giving a valid phase diagram, this curvature model can predict how fluctuation effects and van der Waals-interactions influence amphiphilic phase behavior in excellent agreement with experiments.

Ginzburg–Landau models not only allow to treat binary and ternary systems on the same footing, but also to implement arbitrary geometries. However, when doing so one is often faced with large parameter spaces and numerical solutions. In the third section, we introduce a Ginzburg–Landau model [11, 12] which can account very well for the polymorphism observed experimentally in binary systems and present a new phase diagram [13] which compares very favorably with experiments. In the fourth section, we conclude by comparing the respective virtues of curvature and Ginzburg–Landau models for the modelling of amphiphilic phase behavior.

## 2. Curvature model

When modelling ternary amphiphilic systems within the framework of curvature models, one assumes that the dominant contribution to the free energy comes from the elastic energy of the amphiphilic monolayers which can be calculated from the Canham–Helfrich Hamiltonian [14, 15]:

$$F_{\text{curv}} = \int dA \left\{ 2\kappa (H - c_0)^2 + \bar{\kappa} K \right\} . \quad (1)$$

Here the integration extends over the neutral surface of the amphiphilic monolayer. At every point of the surface one has the mean curvature  $H$  and the Gaussian curvature  $K$ . The spontaneous curvature  $c_0$  reflects the tendency of the monolayer to bend preferably either towards the adjacent oil regions ( $c_0 > 0$ ) or towards the adjacent water regions ( $c_0 < 0$ ). This quantity carries the main temperature dependence of the model since it is found experimentally to vary linearly with temperature [16]:

$$c_0(T) = c_0(T_R) \frac{(T_m - T)}{(T_m - T_R)} , \quad (2)$$

where  $T_R$  denotes the room temperature and  $T_m$  the phase inversion temperature. The bending of the monolayers is governed by the bending rigidity  $\kappa$  which can range from  $1 k_B T$  for tensides like  $C_{12}E_5$  to  $10 k_B T$  for biological lipids like DMPC. It follows from the Gauss–Bonnet theorem that the Gaussian bending rigidity  $\bar{\kappa}$  reflects the energy cost associated with changing topology. Usually it is assumed to have a small negative value. Here we choose  $\bar{\kappa}/\kappa = -0.5$  which suppresses the hexagonal phase  $H_1$  in favor of the micellar disordered phase  $L_1$  [9].

In addition to the curvature energy, we also consider fluctuation effects and the van der Waals-interaction. These contributions to the free energy can be calculated in closed form for the micellar disordered phase  $L_1$  and the lamellar phase  $L_\alpha$  only. Therefore these two phases have been considered in our first study [10]. Fluctuations in the droplet phase can be shown to encompass the usual hard sphere entropy as well as the undulation energy of the single closed monolayers [17]. Fluctuations in the lamellar phase lead to the steric repulsion between adjacent monolayers [18]. The van der Waals-energy is calculated from

$$F_{vdW} = \frac{A}{\pi^2} \int d^3r_1 \int d^3r_2 \left\{ \frac{\varepsilon^2}{[(\mathbf{r}_1 - \mathbf{r}_2)^2 + \varepsilon^2]^4} - \frac{1}{[(\mathbf{r}_1 - \mathbf{r}_2)^2 + \varepsilon^2]^3} \right\} \quad (3)$$

with the Hamaker constant  $A = 1 k_B T$  for the interaction of hydrocarbon across water and the cutoff length  $\varepsilon = 0.7$  (length is measured in units of amphiphile length).

Fig. 2(a) shows two phase diagrams calculated for parameter values characteristic for the system  $H_2O/C_{12}E_5/C_{14}$ . Then  $T_m = 48^\circ C$ ,  $c_0(T_R) = 1/6$  and  $\kappa = 1 k_B T$  [16]. The first phase diagram corresponds to  $T = 20^\circ C$ , the second to  $T = 37^\circ C$ . As temperature is increased, the lamellar phase  $L_\alpha$  extends further and further into the water apex of the Gibbs triangle, in excellent agreement with experiments [4,5]. It follows from our model that the channel of disordered micellar phase  $L_1$  which is observed between the binary side and the lamellar phase is caused by the steric repulsion of the monolayers over the oil regions. Fig. 2(b) shows phase diagrams calculated for higher values of the bending rigidity  $\kappa$  (with  $1/c_0(T) = 15.3$ ). When  $\kappa$  is increased to  $2.8 k_B T$ , the  $L_1$ -channel disappears since the steric repulsion gets weaker. If  $\kappa$  is raised to  $9.5 k_B T$ , the van der Waals-interaction begins to dominate and one finds bound lamellae coexisting with excess water. This prediction is in excellent agreement with experiments on the binary system  $H_2O/DMPC$  [19]. Moreover, here also the lamellae gradually unbind as pentanol is added as cosurfactant which effectively decreases  $\kappa$ . In any of the phase diagrams shown there is another coexistence between the  $L_1$ -phase and the excess oil phase, the so-called *emulsification failure* which is common to all amphiphilic systems.

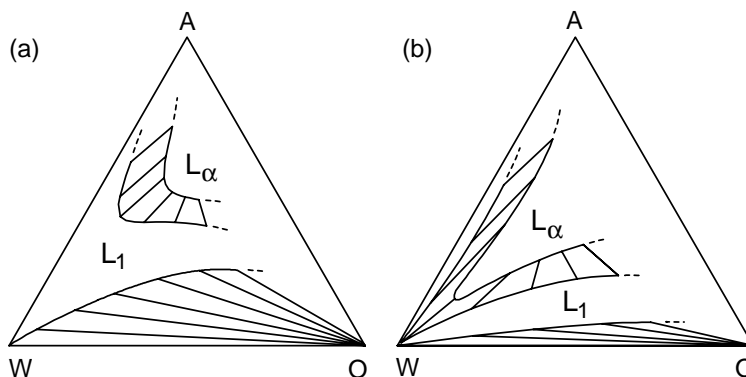


Fig. 2(a) Phase diagrams calculated with the curvature model for low bending rigidity: (a)  $T = 20^\circ\text{C}$  and (b)  $T = 37^\circ\text{C}$ ,  $\kappa = 1 k_{\text{B}}T$ ,  $T_m = 48^\circ\text{C}$  and  $c_0(T_R) = 1/6$ . This choice corresponds to the tenside system  $\text{H}_2\text{O}/\text{C}_{12}\text{E}_5/\text{C}_{14}$ . As temperature is increased, the lamellar phase  $L_\alpha$  stretches further into the water apex while leaving a channel of disordered micellar phase  $L_1$  on the binary side which can be explained with the steric repulsion between monolayers. The coexistence of  $L_1$  with excess oil is known as *emulsification failure*.

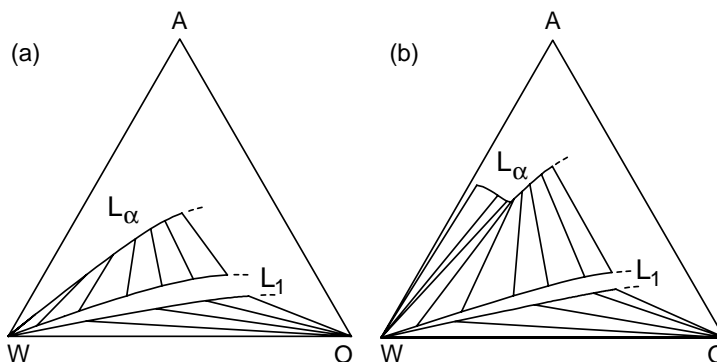


Fig. 2(b) Phase diagrams calculated with the curvature model for high bending rigidity: (a)  $\kappa = 2.8 k_{\text{B}}T$  and (b)  $\kappa = 9.5 k_{\text{B}}T$ ,  $1/c_0(T) = 15.3$ . The latter value corresponds to a lipid system with DMPC. With increasing  $\kappa$ , the  $L_1$ -channel on the binary side disappears. The lamellae then become bound since the steric interaction becomes weaker and the van der Waals-interaction begins to dominate.

### 3. Ginzburg–Landau model

In order to model binary amphiphilic systems within the framework of a Ginzburg–Landau model, we choose to use the amphiphile concentration  $\phi(\mathbf{r})$  and orientation  $\boldsymbol{\tau}(\mathbf{r})$  as appropriate order parameter fields. Here  $|\boldsymbol{\tau}(\mathbf{r})|$  reflects the degree of the amphiphile alignment. Since we assume incompressibility, the water concentration then follows as  $1 - \phi(\mathbf{r})$ . The free energy

functional  $\mathcal{F}[\phi, \boldsymbol{\tau}]$  can be derived either as continuum limit of an appropriate lattice model or from a symmetry analysis. Assuming  $\nabla \times \boldsymbol{\tau}(\mathbf{r}) = 0$ , one finds [11, 12]

$$\mathcal{F}[\phi, \boldsymbol{\tau}] = \int d\mathbf{r} \left\{ \alpha_1 (\nabla \cdot \boldsymbol{\tau})^2 + \alpha_2 (\Delta \boldsymbol{\tau})^2 + \beta_1 (\nabla \phi)^2 + \gamma_1 (\nabla \phi \cdot \boldsymbol{\tau}) + U(\phi, \boldsymbol{\tau}^2) \right\}, \quad (4)$$

where  $U(\phi, \boldsymbol{\tau}^2)$  is the free energy density of the homogeneous phases. Within the Flory–Huggins approximation it is calculated as

$$U(\phi, \boldsymbol{\tau}^2) = a_2 \phi^2 + T(\phi \ln \phi + M(1 - \phi) \ln(1 - \phi)) + b_2 \boldsymbol{\tau}^2 + T\phi \left( c_2 \frac{\boldsymbol{\tau}^2}{\phi^2} + c_4 \frac{\boldsymbol{\tau}^4}{\phi^4} \right). \quad (5)$$

Here  $T$  denotes the reduced temperature and  $M$  the amphiphile molecular volume relative to the water molecular volume. The model describes the usual lower miscibility gap of a binary system for  $a_2 < 0$ . A calculation of correlation functions in the Gaussian approximation shows that  $\alpha_1 < 0$  corresponds to amphiphilic self-assembly. All other parameters are taken to be positive. It is straightforward to derive a similar model for ternary systems when the order parameter field  $\Phi(\mathbf{r})$ , which is the local density difference between oil and water, is considered additionally [13, 20].

Fig. 3 shows a typical phase diagram calculated in mean field approximation [13]. In order to test systematically and efficiently for the stable phase at any given point of the phase diagram, a Fourier ansatz has been

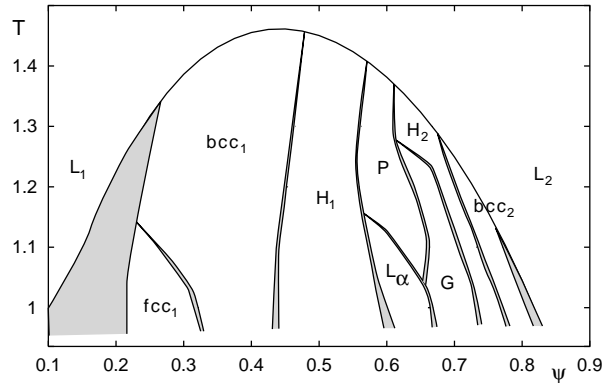


Fig. 3. Phase diagram calculated with the Ginzburg–Landau model in mean field approximation:  $\alpha_1 = -6$ ,  $\alpha_2 = 10$ ,  $\beta_1 = 10$ ,  $\gamma_1 = 30$ ,  $a_2 = -10$ ,  $M = 20$ ,  $b_2 = 1$ ,  $c_2 = 1.4$  and  $c_4 = 1$ . A line of critical points separates the ordered phases at low temperatures from the disordered phase at high temperatures. Phase boundaries are mainly lyotropic and the sequence of phases with increasing amphiphile concentration is as typically observed for systems with  $H_2O$  and  $C_iE_j$ .

used for all relevant ordered phases [21]. Special care has been taken to include various bicontinuous cubic phases which recently have been shown to be accessible by Ginzburg–Landau models [22]. The phase diagram shows a line of critical points separating the ordered phases at low temperatures from the high temperature disordered phase. Following a cut at  $T = 1.0$ , one finds the sequence disordered micellar–fcc–bcc–hexagonal–lamellar–gyroid–inverted hexagonal–inverted bcc–disordered inverted micellar when increasing the amphiphile concentration. This corresponds nicely to experimental results on systems with  $\text{H}_2\text{O}$  and  $C_iE_j$  [2,3]. Note that there are two stable cubic bicontinuous phases: P denotes a structure which results when draping an amphiphilic *monolayer* onto the triply periodic minimal surface P (spacegroup 221). G results when draping an amphiphilic *bilayer* onto the triply periodic minimal surface G (spacegroup 230). The latter structure is known as *double gyroid* from diblock copolymer systems [23] and is depicted in Fig. 4. Since there are different structural types arising from the same triply periodic surface when draped differently with physical entities, one has to make sure not to miss any of these possible phases when testing for the stable phase.

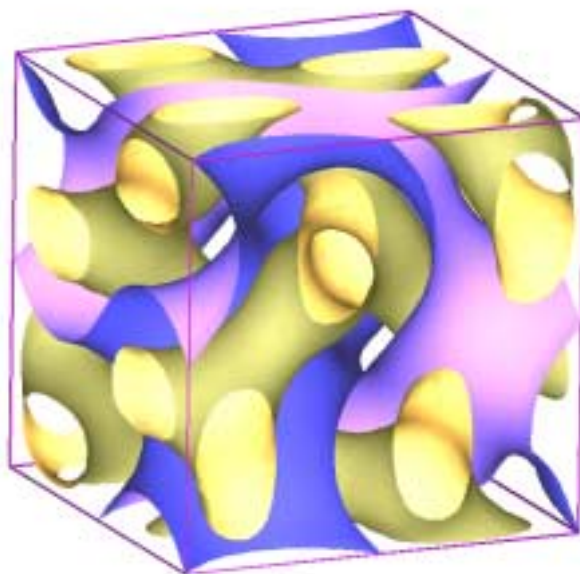


Fig. 4. Visualisation of the double gyroid, which is a stable phase in the phase diagram of Fig. 3. As a guide to the eyes, the triply periodic minimal surface G is shown in dark. Since an amphiphilic bilayer is draped onto it, there are two disconnected, but interwoven water labyrinths which are shown in light. The space group is 230 ( $Ia\bar{3}d$ ).

#### 4. Conclusion

It has been shown here that mesoscopic models like curvature and Ginzburg–Landau models can explain many generic aspects of amphiphilic phase behavior. Curvature models are particularly useful for investigating ternary phase behavior since here even micellar structures are built up from amphiphilic monolayers which are governed by the Canham–Helfrich Hamiltonian. For simple geometries like lamellae and spheres, one can calculate explicitly the effects of fluctuations and long-ranged forces like the van der Waals-interaction. Since curvature models feature only few parameters, comparison with experiments is rather easy. It follows that there are indeed effects on amphiphilic phase behavior which can be observed experimentally: for low bending rigidity  $\kappa$  (*i.e.* tensides), the lamellar phase extends further and further into the water apex of the Gibbs triangle as temperature is increased towards the phase inversion temperature. For high bending rigidity  $\kappa$  (*i.e.* lipids), one finds bound lamellae in coexistence with excess water.

Ginzburg–Landau models can be used to model many different structures both for binary and ternary systems. Although they can be shown to reproduce the Canham–Helfrich Hamiltonian, they only describe short-ranged interactions [6]. Since phase diagrams can be calculated easily only in the mean field approximation, we conclude that they are more appropriate for low temperature behavior where fluctuation effects are less prominent. In fact we showed that they very well predict the typical phase sequence observed for binary systems with  $\text{H}_2\text{O}$  and  $C_iE_j$  when raising the amphiphile concentration. In contrast to curvature models, the relevant geometries are not presupposed but within the mean field approximation are obtained from minimizing the free energy functional. In fact we believe that the broad two-phase regions obtained with the curvature model results from the fact that soft geometries like deformed droplets have not been taken into account.

In conclusion, different aspects of amphiphilic phase behavior can be modeled best by different models. In order to obtain a complete picture, it is therefore impedient to use all models available. In this sense curvature and Ginzburg–Landau models have to be considered to be complementary to each other.

It is a pleasure to thank G. Gompper for very enjoyable collaboration.

## REFERENCES

- [1] W.M. Gelbart, A. Ben-Shaul, D. Roux, *Micelles, Membranes, Microemulsions, and Monolayers*, Springer-Verlag, New York 1994.
- [2] D.J. Mitchell, G.J.T. Tiddy, L. Waring, T. Bostock, M.P. McDonald, *J. Chem. Soc. Faraday Trans.* **79**, 975 (1983).
- [3] R. Strey, R. Schomäcker, D. Roux, F. Nallet, U. Olsson, *J. Chem. Soc. Faraday Trans.* **86**, 2253 (1990).
- [4] H. Kunieda, K.J. Shinoda, *J. Dispersion Sci. Technol.* **3**, 233 (1982).
- [5] U. Olsson, U. Würz, R. Strey, *J. Phys. Chem.* **97**, 4535 (1993).
- [6] G. Gompper, M. Schick, *Self-assembling amphiphilic systems, Phase Transitions and Critical Phenomena*, vol. 16, Academic Press, London 1994.
- [7] M.W. Matsen, M. Schick, D.E. Sullivan, *J. Chem. Phys.* **98**, 2341 (1993).
- [8] R.G. Larson. *J. Phys. II France* **6**, 1441 (1996).
- [9] Z.-G. Wang, S.A. Safran, *Europhys. Lett.* **11**, 425 (1990).
- [10] U.S. Schwarz, K. Swamy, G. Gompper, *Europhys. Lett.* **36**, 117 (1996).
- [11] G. Gompper, S. Klein. *J. Phys. II France*, 2:1725-44, 1992.
- [12] G. Gompper, U.S. Schwarz, *Z. Phys.* **B97**, 233 (1995).
- [13] U.S. Schwarz, G. Gompper, in preparation.
- [14] P.B. Canham, *J. Theor. Biol.* **26**, 61 (1970).
- [15] W. Helfrich, *Z. Naturforsch.* **C28**, 693 (1973).
- [16] R. Strey, *Colloid Polym. Sci.* **272**, 1005 (1994).
- [17] D.C. Morse, S.T. Milner, *Phys. Rev.*, **E52**, 5918 (1995).
- [18] W. Helfrich, *Z. Naturforsch.* **A33**, 305 (1978).
- [19] C.R. Safinya, E.B. Sirota, D. Roux, G.S. Smith, *Phys. Rev. Lett.* **62**, 1134 (1989).
- [20] A. Ciach, *J. Chem. Phys.* **104**, 2376 (1996).
- [21] U. Shmueli (ed.), *International Tables for Crystallography, Volume B: Reciprocal Space*, Kluwer Academic Publishers, Dordrecht (1996).
- [22] W. Gozdz, R. Holyst, *Phys. Rev.* **E54**, 1 (1996).
- [23] M.W. Matsen, F.S. Bates, *Macromolecules* **29**, 1091 (1996).